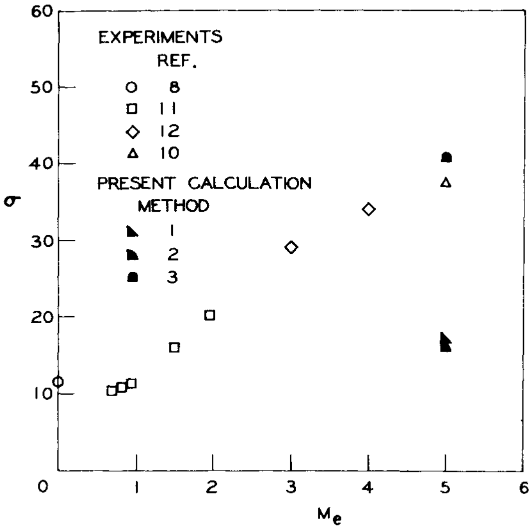

Fig. 4 Spreading parameter.

with a mean-dilatation correction factor and the normal momentum equation. In Method (3), an average value at a given x station, defined as

$$\bar{F}(x) = \int_{y_1}^{y_1} F\, dy/(y_2 - y_1)$$

has been used to avoid numerical difficulties. A typical computed variation of F is shown in Fig. 1 and the corresponding $\bar{F}$ which was used in the calculations. This average $\bar{F}$ was taken only over the portion of the shear layer where momentum diffusion is important as indicated by region between y_1 and y_2 in Fig. 1. Outside of this region the small values of momentum or velocity gradient caused the diffusivity correction to be of no significance in the solution. The value of $\bar{F}$ was found to vary from 0.703 at $x = 7.3$ cm to 0.553 at $x = 24.4$ cm.

Predicted mean axial velocity, static pressure, and spreading parameter σ are shown in Figs. 2–4 respectively.[11,12] σ has been defined by the relation[4] $\sigma = 1.32/\Delta\eta$ where $\Delta\eta$ is the angular distance between two rays η_1 and η_2 defined by $[\tilde{u}(\eta_1) - \tilde{u}_\infty]/(\tilde{u}_e - \tilde{u}_\infty) = (0.1)^{1/2}$ and $[\tilde{u}(\eta_2) - \tilde{u}_\infty]/(\tilde{u}_e - \tilde{u}_\infty) = (0.9)^{1/2}$. The inclusion of the normal mean momentum equation alone, without considering effects of pressure variation on the turbulence structure itself, does not improve the prediction. But simple mixing length theory with a mean dilatation effect correction, though it lacks sound analytical backing, predicts the turbulent free shear layer surprisingly well as can be seen in Figs. 2 and 4. It should be noted that the inclusion of the mean dilatation "correction factor" is in some sense a crude attempt to include the influence of the important $\overline{p' \partial u_i'/\partial x_i}$ term which appears in the compressible form of the turbulent kinetic energy equation. This term is expected to reduce $\overline{u'v'}$ and one would expect that generally $\partial u_i'/\partial x_i$ would be proportional to $\partial \tilde{u}_i/\partial x_i$.

References

[1] Rudy, D. H. and Bushnell, D. M., "A Rational Approach to the Use of Prandtl's Mixing Length Model in Free Turbulent Shear Flow Calculations," *Proceedings of the Conference on Free Turbulent Shear Flows*, NASA SP-321, Vol. 1, 1972, pp. 67–137.

[2] Bushnell, D. M. and Beckwith, I. E., "Calculation of Nonequilibrium Hypersonic Turbulent Boundary Layers and Comparisons With Experimental Data," *AIAA Journal*, Vol. 8, No. 8, Aug. 1970, pp. 1462–1469.

[3] Beckwith, I. E. and Bushnell, D. M., "Calculation by a Finite-Difference Method of Supersonic Turbulent Boundary Layers With Tangential Slot Injection," TN D-6221, April 1971, NASA.

[4] Brown, G. and Roshko, A., "The Effect of Density Difference on the Turbulent Mixing Layer," AGARD CP-93, 1971, pp. 23-1 to 23-12.

[5] Bradshaw, P., "Anomalous Effects of Pressure Gradient on Supersonic Turbulent Boundary Layers," Aero Rept. 72-21, Nov. 1972, Imperial College of Science and Technology, London, England.

[6] Favre, A., "Statistical Equations of Turbulent Gases," *Problems of Hydrodynamics and Continuum Mechanics*, Society for Industrial and Applied Mathematics, Philadelphia, Pa., 1969, pp. 231–266.

[7] Bradshaw, P., "The Turbulence Structure of Equilibrium Boundary Layers," *Journal of Fluid Mechanics*, Vol. 29, Pt. 4, 1967, pp. 625–645.

[8] Liepmann, H. W. and Laufer, J., "Investigations of Free Turbulent Mixing," TN-1257, Aug. 1947, NACA.

[9] Wilcox, D. C. and Alber, I. E., "A Turbulence Model for High Speed Flows," *Proceedings of 23rd Heat Transfer and Fluid Mechanics Institute*, San Fernando Valley State College, North Ridge, Calif., 1972, pp. 231–252.

[10] Morrisette, E. L. and Birch, S. F., "Mean Flow and Turbulence Measurements in a Mach 5 Shear Layer. Part I—The Development and Spreading of the Mean Flow," *Fluid Mechanics of Mixing, ASME*, 1973, pp. 79–81.

[11] Maydew, R. C. and Reed, J. F., "Turbulent Mixing of Axisymmetric Compressible Jet (in the Half Jet Region) With Quiescent Air," Res. Rept. SC-4764 (RR), March 1963, Sandia Corp., Albuquerque, N.Mex.

[12] Sirieix, M. and Solignac, J. L., "Contribution à l'Etude Expérimentale de la Couche de Mélange Turbulent Isobare d'un Encoulement Supersonique," *Symposium on Separated Flow, AGARD* Conference Proceedings No. 4, 1966, pp. 241–270.

Effect of Finite Chemical Reaction Rates on Heat Transfer to the Walls of Combustion-Driven Supersonic MHD Generator Channels

J. W. DAILY*
Stanford University, Stanford, Calif.

AND

J. RAEDER† AND G. ZANKL†
Max-Planck-Institut für Plasmaphysik, Garching, Germany

THE effect of finite-rate homogeneous chemical reactions on heat-transfer rates to rocket nozzles is well known. It has not been widely recognized, however, that these effects may be important in combustion-driven supersonic MHD power generators, where conditions are similar to those in rocket nozzles. Data taken at the Institut für Plasmaphysik in Garching, Germany, and preliminary boundary-layer calculations done at Stanford Univ. indicate a significant reduction in wall heat flux due to finite rate effects.

Finite reaction rates may manifest themselves in two ways. First, the expansion process may be rapid enough to cause freezing in the bulk of the flow; secondly, gradients in the wall boundary layer may be severe enough, especially in turbulent flows, to cause freezing in the wall region. Comparison of reaction times[1] and the various flow characteristic times indicates that it is the latter case which is likely to occur for the experiments considered here.

Received August 24, 1973. The computer work reported was supported by AFAPL Contract F33615-72-C-1088.

Index categories: Boundary Layers and Convective Heat Transfer—Turbulent; Plasma Dynamics and MHD; Electric Power Generation Research.

* Research Assistant, High Temperature Gasdynamics Laboratory, Mechanical Engineering Department.

† Research Scientist.

Table 1 Data of the combustion MHD generator

Fuel	JP-1
Oxydator	liquid oxygen
Seed material	potassium octoate (C_7H_{15}-COOK)
Seed rate	3% by weight of K in fuel + seed mat.
Total mass flow rate	1.5 kg/s
Combustion chamber	
Pressure	15 bar
Channel entrance	
Pressure	4.5 bar
Gas temperature	2850 K
Mach number	1.5
Cross-sectional area	20 cm^2
Distance from nozzle throat	11 cm
Channel exit	
Cross-sectional area	60 cm^2
Channel length	1.6 m

The experiments were performed on the 200 kW$_{el}$ combustion MHD generator of the IPP-MAN association.[2] The data of the facility are presented in Table 1.

The channel, of the Hall type with circular cross section, was composed of axially segmented copper disks (9.5-mm thick). These segments were isolated both electrically and thermally from each other with 0.5-mm-thick insulating foils.

The density of the heat flux to the wall q_w was measured for various axial positions via the temperature increase in the channel wall as a function of time. All measurements were performed without an applied magnetic field. The measured values of q_w are plotted vs the distance x from the nozzle throat in Fig. 1.

Measurements were also performed with a diagonal wall channel with rectangular cross section. The entrance and exit cross-sectional areas and the length of this channel are the same as for the circular one. All the other data were very similar in the experiments with both channels. The values of q_w measured in the rectangular channel are also presented in Fig. 1.

A limit study was performed at Stanford for the conditions of the IPP experiment using the Patankar-Spalding[3] turbulent boundary-layer program. For comparison with the experimental values the results for the equilibrium and frozen limits in the case of a round channel are plotted in Fig. 1. (Rectangular channel results are virtually identical.) The behavior of the two theoretical distributions of q_w directly reflects the influence of the specific heat c_p. For the temperature at the channel entrance ($T \simeq 2850$ K) the finite-rate effect leads to a large difference between $c_{p,\text{frozen}}$ and $c_{p,\text{equ.}}$, whereas for the temperature in the exit region ($T \simeq 2500$ K) this difference is small. As can be seen, the data indicate that measured heat-transfer rates fall close to the frozen limit. It should be noted that catalytic wall effects would raise the heat transfer rate.

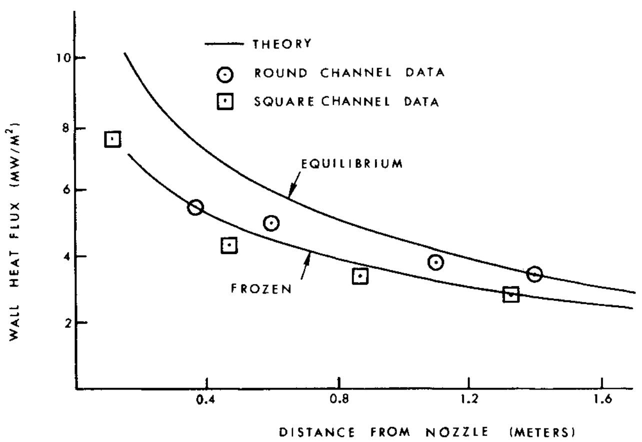

Fig. 1 Heat flux along the walls of the IPP-MAN round and square channels.

In conclusion, a substantial decrease in heat-transfer rate to the walls of a combustion-driven supersonic MHD power generator was observed which appears to occur because of chemical nonequilibrium in the developing wall boundary layers.

References

[1] Newhall, H. K., "Kinetics of Engine Generated Nitrogen Oxides and Carbon Monoxide," *12th Symposium (International) on Combustion*, Poitiers, France, 1968.

[2] Bünde, R. et al., "Theoretical, Experimental, and Technical Investigations for the Development of a Pulsed Combustion MHD Generator," *Proceedings of the 5th International Conference on MHD Electric Power Generation*, Vol. 1, IAEA, Munich, 1971, p. 229.

[3] Patankar, S. V. and Spaulding, D. B., *Heat and Mass Transfer in Boundary Layers*, 2nd Ed., International, London, 1970.

Torque Development on a Spherical Body due to Spin Up of the Concentric Spherical Container

RAM SINHA*

The Singer Company, Kearfott Division, Little Falls, N.J.

Nomenclature

A = a function as defined in Eq. (24)
D = a parameter as defined in Eq. (28)
h = gap height between the two spheres, $R_o - R_i$
k = a parameter defined as $(\alpha/2\nu)^{1/2}$
N = viscous torque on the inner sphere
n = an integer variable
R_i = radius of the inner sphere
R_o = radius of the outer sphere
r = radial coordinate
t = time
v_r = velocity component in r-direction
v_θ = velocity component in θ-direction
v_ϕ = velocity component in ϕ-direction
x = $r - R_i$
z = Cartesian z-coordinate, selected along the axis of rotation of the spherical container
α = frequency in radians per unit time
β = $n\pi/h$
δ = a parameter defined in Eq. (29)
ε = phase angle in the harmonic motion of the spherical container
θ = angle θ in spherical coordinates
μ = viscosity of fluid
ν = kinematic viscosity, μ/ρ
ξ = a dummy variable for integration
ρ = density of fluid
τ = shear stress in fluid
ϕ = angle ϕ in spherical coordinates
ψ = a function as defined in Eq. (25)
Ω = angular speed of the outer sphere
Ω_o = maximum value of Ω
ω = angular speed of the fluid

Subscripts

r = r-direction in spherical coordinates
θ = θ-direction in spherical coordinates
ϕ = ϕ-direction in spherical coordinates

Received September 6, 1973.

Index categories: Viscous Nonboundary-Layer Flows; LV/M Guidance Systems (Including Command and Information Systems); Spacecraft Attitude Dynamics and Control.

* Senior Scientist—Fluidics, Research Center, Aerospace and Marine Systems Group; presently Research Engineer, Scientific Analysis Group, Pratt & Whitney Aircraft, East Hartford, Conn.